A Bootstrapped Modularised method of Global Sensitivity Analysis applied to Probabilistic Seismic Hazard Assessment

Francesco Di Maio[a], Nicola Gallo[a], Daniele Arcangeli [c], Matteo Taroni [d], Jacopo Selva[e], Enrico Zio[a,b]
[a] Energy department, Politecnico di Milano, Milan, Italy
[b] MINES ParisTech, PSL Research University, CRC, Sophia Antipolis, France
[c] Universita' di Bologna Alma Mater Studiorum, Dipartimento di Fisica e Astronomia "Augusto Righi", Bologna, Italy
[d] Istituto Nazionale di Geofisica e Vulcanologia, Sezione di Roma 1, Rome, Italy
[e] Istituto Nazionale di Geofisica e Vulcanologia, Sezione di Bologna, Bologna, Italy

ABSTRACT

Probabilistic Seismic Hazard Assessment (PSHA) evaluates the probability of exceedance of a given earthquake intensity threshold like the Peak Ground Acceleration, at a target site for a given exposure time. The stochasticity of the occurrence of seismic events is modelled by stochastic processes and the propagation of the earthquake wave in the soil is typically evaluated by empirical relationships called Ground Motion Prediction Equations. The large uncertainty affecting PSHA is quantified by defining alternative model settings and/or model parametrizations. In this work, we propose a novel Bootstrapped Modularised Global Sensitivity Analysis (BMGSA) method for identifying the model parameters most important for the uncertainty in PSHA, that consists in generating alternative artificial datasets by bootstrapping an available input-output dataset and aggregating the individual rankings obtained with the modularized method from each of those.

The proposed method is tested on a realistic PSHA case study in Italy. The results are compared with a standard variance-based Global Sensitivity Analysis (GSA) method of literature. The novelty and strength of the proposed BMGSA method are both in the fact that its application only requires input-output data and not the use of a PSHA code for repeated calculations.

Keywords: Probabilistic Seismic Hazard Assessment (PSHA), uncertainty, Modularised Global Sensitivity Analysis (MGSA), Bootstrapped Modularised Global Sensitivity Analysis (BMGSA)

Acronyms

PSHA	Probabilistic Seismic Hazard Assessment
PGA	Peak Ground Acceleration
GMPE	Ground Motion Prediction Equation
SA	Sensitivity Analysis
GSA	Global Sensitivity Analysis
MGSA	Modularised Global Sensitivity Analysis
BMGSA	Bootstrapped Modularised Global Sensitivity Analysis
IM	Intensity Measure
MCS	Monte Carlo Simulation
BU	Bottom-Up
AO	All-Out
BC	Borda Count

Symbols

$\boldsymbol{\gamma}$	Threshold value of the given intensity measure
$\boldsymbol{\lambda_H}$	Annual rate of exceedance of the $\boldsymbol{\gamma}$-th PGA level
$\boldsymbol{\lambda}$	Annual rate of main shock occurrence at a given source location
$\boldsymbol{f_m(m)}$	Probability distribution of different earthquake magnitudes
$\boldsymbol{m_{min}}$	Minimum magnitude of the probability distribution $\boldsymbol{f_m(m)}$
$\boldsymbol{m_{max}}$	Maximum magnitude of the probability distribution $\boldsymbol{f_m(m)}$
$\boldsymbol{b}$	Slope parameter of the probability distribution $\boldsymbol{f_m(m)}$
$\boldsymbol{f_r(r)}$	Probability distribution of the source-to-target distance
$\boldsymbol{r}$	Source-to-target distance
$\boldsymbol{C}$	Computational cost of the double-loop Monte Carlo Simulation
$\boldsymbol{v}$	Number of input variables

$\boldsymbol{n_1}$	Sample size for estimating the inner loop of the double-loop MCS
$\boldsymbol{n_2}$	Sample size for estimating the outer loop of the double-loop MCS
$\boldsymbol{d}$	Index of the generic bootstrapped dataset
$\boldsymbol{D}$	Total number of the bootstrapped dataset
$\boldsymbol{g}$	Model
$\boldsymbol{Y}$	Output of the model $\boldsymbol{g}$
$\overline{\boldsymbol{X}}$	Input parameters
$\overline{\overline{\boldsymbol{Z}}}$	Input-output dataset
$\boldsymbol{s}$	Index of the input-output pattern of $\overline{\overline{\boldsymbol{Z}}}$
$\boldsymbol{S}$	Total number of the input-output pattern of $\overline{\overline{\boldsymbol{Z}}}$, i.e., number of rows of $\overline{\overline{\boldsymbol{Z}}}$
$\boldsymbol{N}$	Number of input parameters, i.e.
$\boldsymbol{n}$	Index of the input parameter
$\boldsymbol{Var}[\cdot]$	Variance
$\mathbb{E}[\cdot]$	Expectation operator
$\boldsymbol{S_n}$	Sobol index of the $\boldsymbol{n}$-th parameter
$\overline{\overline{\boldsymbol{Z}}}_{\boldsymbol{d}}^{*}$	Reduced matrix
$\boldsymbol{K}$	Number of mutually exclusive subset of the reduced matrix
$\boldsymbol{k}$	Index of the mutually exclusive subsets of the reduced matrix
$\overline{\overline{\boldsymbol{Z}}}_{\boldsymbol{d}}^{*\boldsymbol{k}}$	Generic mutually exclusive subset of the reduced matrix of the generic bootstrapped dataset
$\boldsymbol{J}$	Number of rows of the $\overline{\overline{\boldsymbol{Z}}}_{\boldsymbol{d}}^{*\boldsymbol{k}}$
$\boldsymbol{S_{n,d}}$	Sobol index of the $\boldsymbol{n}$-th parameter of the generic $\boldsymbol{d}$-th bootstrapped dataset
$\overline{\boldsymbol{R}}_{\boldsymbol{BU,d}}$	Input ranking (bottom-up strategy) of the generic bootstrapped dataset
$\overline{\boldsymbol{R}}_{\boldsymbol{BU}}$	Final aggregated input ranking (bottom-up strategy)
$\boldsymbol{BC_n}$	Borda count for the $\boldsymbol{n}$-th input variable
$\boldsymbol{p_{n,d}}$	$\boldsymbol{n}$-th input variable order inside the $\boldsymbol{d}$-th ranking
$\overline{\boldsymbol{R}}_{\boldsymbol{AO}}$	Final aggregated input ranking (all-out strategy)
$\boldsymbol{\sigma_{GMPE}}$	Standard deviation of the GMPE

1. INTRODUCTION

Probabilistic Seismic Hazard Assessment (PSHA) consists of assessing at a given target location and for a given exposure time window, the probability that a given intensity measure (IM) of the ground motion, typically the Peak Ground Acceleration (PGA), exceeds a threshold value γ, that is then summarized in hazard curves, where the IM is plotted versus its annual rate of exceedance [1]. To compute the annual rate of exceedance, the most consolidated and widely used method is described in [2]: first, the annual rate of the mainshocks (i.e., the largest magnitude events in a seismic sequence) is estimated; then, the propagation of the ground motion from the source to the site of interest is performed. Usually, the former is based on an Earthquake Rupture Forecast model, that relies on either spatial distributions of the mainshocks, commonly using area source models [3], or smoothed seismicity models [4] and grid-seismicity source model [5]and [6], coupled with magnitude frequency distributions, ordinarily derived by the Gutenberg-Richter law [7].

The propagation of the ground motion is typically evaluated by empirical relationships, called Ground Motion Prediction Equations (GMPEs), finally leading to the annual rate of exceedance of a selected IM level, λ_H, that is quantified by means of the total probability theorem as [8]:

$$\lambda_H(PGA > \gamma) = \lambda \int_{m_{min}}^{m_{max}} \int_{0}^{R_{max}} P(PGA > \gamma | m, r) f_m(m) f_r(r) dm dr \quad (1)$$

where λ is the annual rate of mainshock occurrence at a given source location (i.e., the number of earthquakes above a given minimum magnitude threshold m_{min} per year); the distribution $f_m(m)$ describes the probability distribution of different earthquake magnitudes, typically assumed to follow a truncated Gutenberg-Richter distribution within the interval of values $[m_{min}; m_{max}]$ and slope parameter b [8]; $f_r(r)$ describes the probability distribution of the source-to-target distance r, assuming a spatial distribution for earthquakes [1]. These input distributions are typically determined from historical, instrumental, and geological observations [1], [9] but large uncertainty

exists, so that many alternative parametrisations of the model are possible [10], [11]. In this respect, Sensitivity Analysis (SA) can aid the understanding of how the uncertainty in the model is apportioned among the model input parameters uncertainties [12], [13]. In other words, through SA, one can identify the most sensitive parameters and better focus the uncertainty analysis without losing accuracy [14]. Different SA techniques have been proposed in literature, which can be sorted into three main categories: local, regional, and global [15]. Local and regional analyses limit inputs variations to a subset of their overall ranges. Local methods evaluate at low computational costs the effects on the system response of small perturbations in the model input variables around fixed values [15]. Then, local SA provides information on the sensitivity of the model output to the input variability at some fixed points. Regional analyses, on the contrary, focus on calculating the sensitivity of the model output to the variability of the inputs varying in given ranges of the inputs; yet, they do not give complete account to the uncertainty of the model inputs, in terms of their distributions [16], [17]. Global Sensitivity Analysis (GSA) methods, instead, explore the whole distribution range of the model inputs and the effects of their mutual combination on the model output, but they do so at larger computational costs than local and regional methods [16], [17]. GSA methods can be regression-based [18], variance-based [17], [19], [20] distribution-based [21], [22] and expected value of information (EVI)-based [23]. Among the GSA methods, variance decomposition based on Sobol indices is most widely used [24].

Sobol indices measure the contribution the input variables provide, individually or in groups, to the variability of the model output [16], [25]. They are usually computed via a double-loop Monte Carlo Simulation (MCS), with computational cost equal to $C = v \cdot n_1 \cdot n_2$, where v is the number of input variables, n_1 the sample size for estimating the inner loop and n_2 the sample size for the outer loop [26], [27]. When the model runs are time consuming, the computational cost is high and strategies have been proposed to reduce it, including: reduced order models calibrated on input-output data

obtained by few runs of the original model, e.g., Bayesian approaches [28], kriging [14], [29],and polynomial chaos expansion [30], [31]; sampling schemes tailored to efficiently characterize the sensitivity of the model inputs, e.g., Fourier Amplitude Sensitivity Test (FAST) [32], [33] and Effective Algorithm for computing global Sensitivity Indices (EASI) [34]; Despite these methods have been successfully applied in many fields, these still raise concern of interpretability within the seismic analysis community when used for PSHA; rather, data-driven approaches, whose data are collected only with the original mode, seems to be more suitable for PSHA, since they allow exploiting available datasets to calculate sensitivity measures [24], [35], [36], [37], which, in general, is quite of interest for many practical applications in which an input-output dataset is available and models to perform a GSA using MCS-based methods cannot be run [24], [38].

In this work, we propose a novel data-driven method based on bootstrapping, Modularised GSA (MGSA) and ensemble strategies, to identify the input variables of a seismic model (for example, $\bar{X} = (\sigma_{GMPE}, \lambda, m_{max}, m_{min}, b, r)$**,** where σ_{GMPE} is the standard deviation of the residual of the GMPE, λ is the annual rate of seismic activity at the source location, m_{min} and m_{max} are the minimum and the maximum magnitude parameters of the truncated Gutenberg-Richter distribution, whose slope is b [8], [39], and r is the source-to-target distance [8]) whose output $Y = \lambda_H(PGA > \gamma)$ is most sensitive to, assuming that only an input-output dataset is given and with no need of repeating hazard computations. The method can be used a posteriori, i.e., when the PSHA has been performed, as well as a priori, when an update of the PSHA is required, by informing the seismologists about the parameters that drive most the uncertainty, and allowing for scenarios exploration, saving modelling efforts and computational time. The procedure of the novel method is sketched in the flowchart of Figure 1. It consists of, first, applying a Bootstrap technique to the available input-output dataset $[\bar{X};\ Y]$ to artificially increase the amount of data available [40], [41]. Then, for each d-th dataset, a sensitivity index is calculated for each input variable. Without loss of

generality, in this work we propose to calculate the first-order Sobol index, which measures the input variables individual contributions to the variability of the model output [16], [25]: in practice, for each input variable, the d-th dataset is modularised (i.e., partitioned) into sub-sets that are used to calculate the variance of the model output Y and the first-order Sobol index [27]. Finally, the D independent rankings of the input variables, obtained based on their first-order Sobol indices values, are ensembled to provide an aggregated ranking of the input variables which the output is sensitive to. Typical ensemble strategies are Bottom-Up (BU) and All-Out (AO) strategies: the former computes a ranking order of the input variables out of each d-th dataset and combines the D alternative rankings a posteriori to generate a final aggregated ranking order [12]; on the contrary, the latter merges a priori the information from the D datasets by averaging the D Sobol indices for each input parameter and, then, provides the final ranking [12].

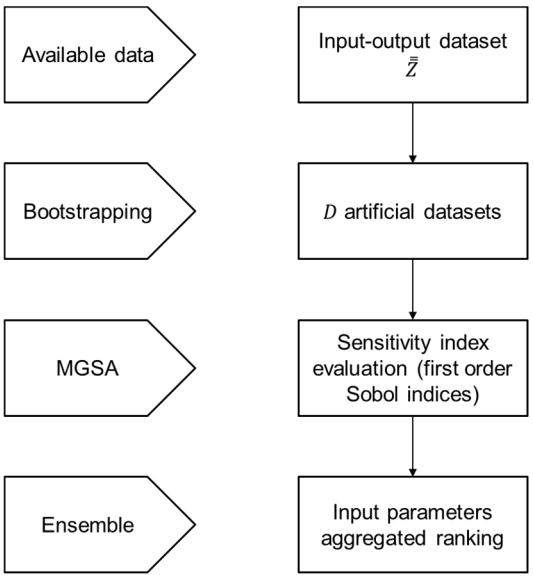

Figure 1 – Flowchart of the proposed method.

The proposed method is tested with respect to the calculation of the hazard intensity corresponding to 10% probability of being exceeded in 50y for a realistic case study with a point seismic source nearby the target site. The results are compared to those obtained by a standard variance-based GSA method [13], which is the state-of-practice approach when the simulation model is available.

The remainder of the paper is organised as follows. Section 2 explains the novel BMGSA method. Section 3 presents the case study. Section 4 shows the results of the application of the proposed method to the data of the case study and the comparison with the results obtained with the standard variance-based GSA of literature. Conclusions are drawn in Section 5.

2. THE NOVEL BOOTSRAPPED MODULARISED GSA

Let us consider a seismic model g whose output value $Y \in \mathbb{R}$ depends on the values of uncertain input parameters $\bar{X} = (X_1, X_2, \dots, X_N)$, with *N* being the number of input parameters:

$$Y = g(\bar{X}) \tag{2}$$

where, without loss of generality, $\bar{X} = (\sigma_{GMPE}, \lambda, m_{max}, m_{min}, b, r)$ and $Y = \lambda_H(PGA > \gamma)$.

Let us also assume that an input-output data set $\bar{\bar{Z}}$ is given (i.e., the analyst may not have the simulation code available):

$$\bar{\bar{Z}} = \begin{pmatrix} \bar{Z}^1 \\ \vdots \\ \bar{Z}^S \end{pmatrix} = \begin{pmatrix} x_1^1 & \cdots & x_N^1 & y^1 \\ \vdots & \ddots & \vdots & \vdots \\ x_1^S & \cdots & x_N^S & y^S \end{pmatrix} \tag{3}$$

where $\bar{Z}^s = [\bar{x}^s, y^s], \forall\, s = 1, \dots, S$ is the s-th input-output pattern of $\bar{Z} = (X_1, X_2, \dots, X_N, Y)$.

The proposed methodology consists in:

1. Generating D alternative bootstrapped artificial datasets from the available input-output dataset $\bar{\bar{Z}}$ [43];
2. From each d-th alternative dataset and for each input variable, calculating a sensitivity index (here the first-order Sobol index) with the modularised method [27];
3. Aggregating the D individual rankings (one for each alternative dataset) with Bottom-Up/All-Out strategies [12].

GENERATION OF THE BOOTSTRAPPED DATASETS

Bootstrap is a computer-based method usually employed to assess the accuracy of statistical estimates with minimum assumptions [41]. The main benefit is avoiding additional computational burden (for example, when simulation codes are computationally demanding or not available, as in the current case) by relying only on the available data [41], [44], which makes it particularly fit for the purpose of this work.

The basic idea is to generate a number D of artificial datasets $\bar{\bar{Z}}_d$ by random sampling, with replacement from $\bar{\bar{Z}}$, the input-output patterns. The generic bootstrapped $\bar{\bar{Z}}_d$, thus, consists in a $S \times (N+1)$ matrix.

THE MODULARISED METHOD TO CALCULATE THE SOBOL INDEX

The Sobol index is the result of the application of a variance-based method that apportions the output variance into the single (or groups of) variables variances [45], [46]. No hypotheses are made on the structure of the model g from which the data have been generated. The variance $Var[Y]$ of the output Y can be, indeed, decomposed as follows [16], [17]:

$$Var[y] = Var_{X_n}\left[\mathbb{E}_{X_{\sim n}}(y|x_n)\right] + \mathbb{E}_{X_n}\left[Var_{X_{\sim n}}(y|x_n)\right] \tag{4}$$

where:

- $Var_{X_n}\left[\mathbb{E}_{X_{\sim n}}(y|x_n)\right]$ is the variance of Y caused by X_n without considering its interactions with other input variables (i.e., $X_{\sim n}$)
- $\mathbb{E}_{X_n}\left[Var_{X_{\sim n}}(y|x_n)\right]$ is the variability of Y depending on all variables but on n (i.e., $X_{\sim n}$);
- $\mathbb{E}(\cdot)$ is the expectation operator;

The first-order Sobol index for the n-th generic input variable is defined as [16], [17] :

$$S_n = \frac{Var_{X_n}\left[\mathbb{E}_{X_{\sim n}}(y|x_n)\right]}{Var[y]}, \forall\, n = 1, \dots, N \tag{5}$$

The larger S_n, the more X_n contributes to the variance of Y [45]. As mentioned in the Introduction, the computation of the Sobol indices usually requires a double-loop MCS, which can be computationally burdensome. Since, in practice, the numerator is solved by a double-loop MCS [17]:

- The inner loop computes $\mathbb{E}_{X_{\sim n}}(y|x_n)$ using n_1 random samples of $\bar{X}_{\sim n}$ with fixed $\bar{X}_n$;
- The outer loop computes $Var_{X_n}\left[\mathbb{E}_{X_{\sim n}}(y|x_n)\right]$ by iterating the inner loop n_2 times, with different values of X_n;

In total, for each S_n, the number of model evaluations is $C_n = n_1 \cdot n_2$, that is unaffordable if each evaluation is time-consuming (notice that, in many practical applications, each loop must be of order greater than 1000 [15], [27]). To address this issue and avoid calling the simulation code, we propose a modularised approach, that partitions the $\bar{\bar{Z}}_d$ into subsets and proceeds as follows [26], [27].

Step 1: construct the reduced matrix

For each n-th input variable, append the n-th input column of $\bar{\bar{Z}}_d$ to the output column; then, shuffle the rows in ascending order to obtain $\bar{\bar{Z}}_d^*$, where $x_n^{1*} \leq x_n^{2*} \leq \cdots \leq x_n^{S*}$:

$$\bar{\bar{Z}}_d^* = \begin{pmatrix} x_n^{1*} & y^{1*} \\ \vdots & \vdots \\ x_n^{S*} & y^{S*} \end{pmatrix} \tag{6}$$

Step 2: partition the reduced matrix in subsets

Partition the support of X_n in $k = 1, \dots, K$ mutually exclusive subsets $\bar{\bar{Z}}_d^{*k}$, such that $\bigcup_{k=1}^{K} X_n^k = X_n \wedge X_n^k \cap X_n^{l \neq k} = \emptyset$. Operatively, divide the resulting matrix $\bar{\bar{Z}}_d^*$ into $k = 1, \dots, K$ submatrices $\bar{\bar{Z}}_d^{*k}$ of J rows, each retaining the order of the Step 1:

$$\bar{\bar{Z}}_d^{*k} = \begin{pmatrix} x_n^{1*k} & y^{1*k} \\ \vdots & \vdots \\ x_n^{J*k} & y^{J*k} \end{pmatrix} \tag{7}$$

Note that $J \cdot K = S$, where S is the total input-output pattern size and $K = int(\sqrt{S})$ [26], [35]. Notice that the large K improves the accuracy of the estimation of $Var_{X_n}[\cdot]$, while worsening the accuracy of the estimation of $\mathbb{E}_{X_{\sim n}}(y|x_n)$, and vice versa [26] [47].

Step 3: estimation of the Sobol index

The Sobol index $S_{n,d}$ is, finally, calculated as in Eq. (8):

$$S_{n,d} = \frac{Var_{X_n}\left[\mathbb{E}_{X_{\sim n}}(y|x_n)\right]}{Var[y]} \approx \frac{\frac{1}{K}\sum_{k=1}^{K}(\bar{y}_k - \bar{y})^2}{\frac{1}{S}\sum_{s=1}^{S}(y_s - \bar{y})^2} \tag{8}$$

where: $\bar{y} = \frac{1}{S}\sum_{s=1}^{S} y^s$ and $\bar{y}_k = \frac{1}{J}\sum_{j=1}^{J} y^{j*k}$.

The calculation of $S_{n,d}$, as a result of the modularisation, depends solely on X_n and Y, and can be performed even if the input values of $\bar{X}_{\sim n}$ are not available [26], [27].

ENSEMBLE OF THE ALTERNATIVE RANKINGS

Each input variable X_n has been, thus, assigned a $S_{n,d}$. Input variables can, accordingly, be ranked from the most important (largest $S_{n,d}$) to the least contributor to the variance (smallest $S_{n,d}$). Two strategies are explored for ensembling the D available alternative rankings: the BU and AO strategies [12].

2.3.1 BOTTOM-UP STRATEGY

Each d-th bootstrapped dataset $\bar{\bar{Z}}_d$ is treated separately from the others to generate its input ranking $\bar{R}_{BU,d}$. Then, the set of input rankings obtained from all the D datasets is processed a posteriori to give the final aggregated ranking order $\bar{R}_{BU}$ (Figure 2) [12] . For each $\bar{\bar{Z}}_d$ the $S_{n,d}$ are computed and, by sorting in ascending order, the corresponding ranking $\bar{R}_{BU,d}$ is obtained. The final ranking order $\bar{R}_{BU}$ is obtained applying the Borda method, that consists in computing the Borda

Count (BC) for each input variable [12]. Denoting by $p_{n,d}$ the n-th variable order inside the d-th ranking, the BC for the input variable X_n is given by [12] :

$$BC_n = \sum_{d=1}^{D} p_{n,d}. \tag{9}$$

A small value of BC_n means that the n-th input variable is among the most important (top ranked) input variables [12].

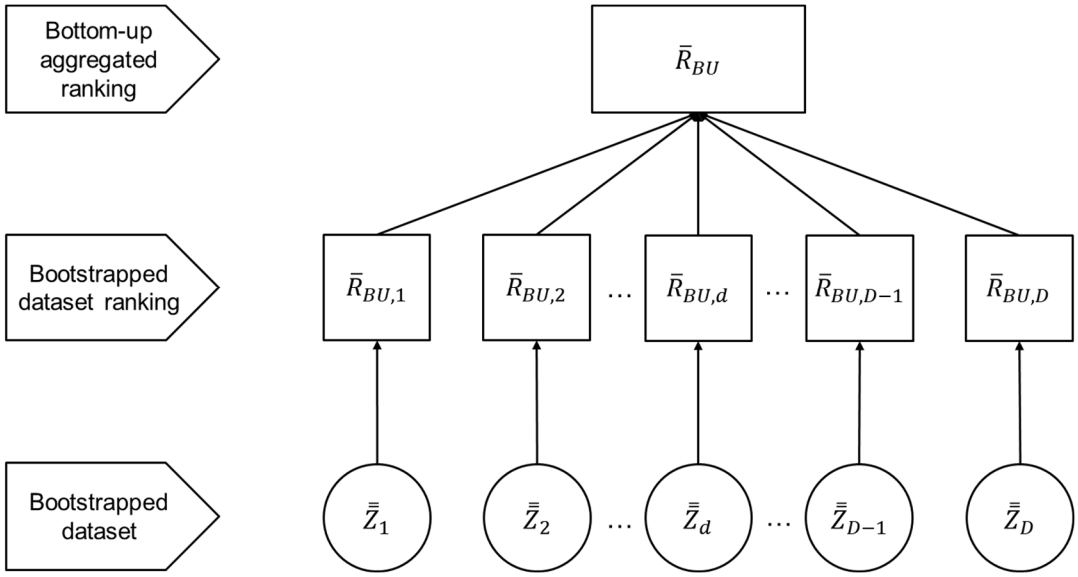

Figure 2 – The proposed bottom-up aggregation strategy.

2.3.2 ALL OUT STRATEGY

The AO strategy a priori merges the information coming from each dataset $\bar{\bar{Z}}_d$. For each input variable X_n, the expected value $\mathbb{E}(S_n)$ of each Sobol index S_n is computed over the D datasets [12]:

$$\mathbb{E}(S_n) = \frac{1}{D}\sum_{d=1}^{D} S_{n,d} \tag{10}$$

Sorting $\mathbb{E}(S_n)$ in ascending order provides the AO aggregated ranking $\bar{R}_{AO}$ (the larger the value of $\mathbb{E}(S_n)$, the more important the n-th input variable) [12].

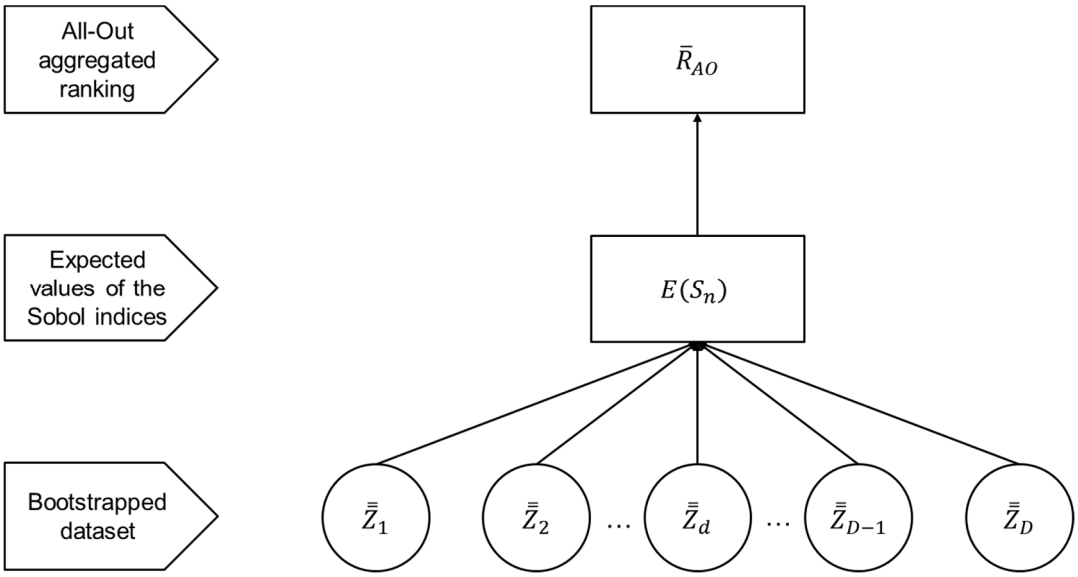

Figure 3 –The proposed all-out aggregation strategy.

3. CASE STUDY

The proposed GSA methodology has been tested on a benchmark case study regarding the PSHA of one hypothetical seismic point source and one target site located in its proximity. Such configuration is of particular interest for zones characterized by short source-to-site distance and high *b*-values (e.g. geothermal filed, volcanic zones, and volcanic islands, [42]).

The source model consists of a point source with a given annual rate and generating seismicity with magnitudes following a truncated Gutenberg-Richter distribution [39]. The source model is, then, coupled with a standard Ground Motion Prediction Equation (GMPE) for the propagation of the earthquake waves [48]. Alternatively, since the target is sited in a volcanic area, other GMPEs might be used, such as those in [49]. A reference target site is selected in the near field, at distance of approximately 10 km.

The uncertainty of the exceedance rate is evaluated by means of Eq. (1) with respect to six input parameters, accounting for a reasonable large number of 16384 alternative computational settings (i.e. 2^{14}, possibly larger than in [13], where, as done in this work, a classical crude Monte Carlo

sampling strategy is used to sample 2^{12} alternative settings), capable of guaranteeing a thorough enough scenario exploration within a tractable computational time. This results in $\bar{\bar{Z}} = [16384 \times 7]$, as in Eq. (11) below. The purpose is to quantify the impact of these parameters on the uncertainty of the IM value corresponding to an exceedance probability of 10% in 50 years, that is with a return period of 475 years. The input parameters are $\bar{X} = (\sigma_{GMPE}, \lambda, m_{max}, m_{min}, b, r)$**.** It is worth mentioning that r is here added to the other typically considered five inputs to emulate the dependence of GMPEs on source characteristics like earthquake depth, size or geometry. The output variable is the PGA, i.e., the reference peak ground acceleration at the target location that has annual rate of exceedance λ_H assumed to be equal to 1/475 (corresponding in this case to a PGA of 0.07g).

$$\bar{\bar{Z}} = \begin{pmatrix} \sigma_{GMPE_1} & \lambda_1 & m_{max_1} & m_{min_1} & b_1 & r_1 & PGA_1 \\ \vdots & \vdots & \vdots & \vdots & \vdots & \vdots & \vdots \\ \sigma_{GMPE_S} & \lambda_S & m_{max_S} & m_{min_S} & b_S & r_S & PGA_S \\ \vdots & \vdots & \vdots & \vdots & \vdots & \vdots & \vdots \\ \sigma_{GMPE_S} & \lambda_S & m_{max_S} & m_{min_S} & b_S & r_S & PGA_S \end{pmatrix} \tag{11}$$

The distributions of all the six input variables $\bar{X}$ are reported in Table 1, all assumed to be normal as customary [13]. Notably, the source-target distance is set around 10 km, thus in the very near field, in which the dependence of distance on the source characteristics (geometry, depth, and dimension) is more pronounced. Consequently, a quite large variance is set for r. The parameters are inspired from the ones adopted in the areal sources of the PSHA study that is enforced by law in Italy, MPS04 [50], [51]. In particular, the parameters of the source model ($\lambda, m_{min}, m_{max}$ and b) are inspired by source zone 920 (Val di Chiana-Ciociaria) of MPS04, with a reduced value m_{min} (from 4.76 to 4.5) and λ (as we are considering a point source). The central value of σ_{GMPE} is instead taken from [48]. Variance value representing the uncertainty on the parameters, are set based on expert judgement.

Table 1 - Model input variables and output, with their associated distributions.

Input variable	Units	Type of distribution	Mean value	Standard deviation
$\boldsymbol{\sigma_{GMPE}}$	$g_0\ (m/s^2)$	Normal	0.3446	0.0490
$\boldsymbol{\lambda}$	yr^{-1}	Normal	0.0600	0.0021
$\boldsymbol{m_{max}}$	-	Normal	5.6791	0.2430
$\boldsymbol{m_{min}}$	-	Normal	4.5005	0.1000
$\boldsymbol{b}$	-	Normal	1.9597	0.0580
$\boldsymbol{r}$	km	Normal	10.0142	2.9639

The results of the proposed method are compared to those obtained by a standard variance-based GSA method [13], which is the state-of-practice approach when the simulation model is available.

4. RESULTS

The BMGSA methodology described in Section 2 has been applied to the case study presented in Section 3. The original dataset $\bar{\bar{Z}}$ has been replicated by bootstrap to generate $D = 1000$ datasets. Each replicate matrix $\bar{\bar{Z}}_d$ is comprised of $S = 16384$ rows (the input-output patterns) and 7 columns (6 input variables, 1 output). The partition size chosen to test the proposed methodology is $K = int(\sqrt{S}) = 128$.

The results of the assessment carried out with the standard GSA on the case study of Section 3 are taken as a benchmark, i.e., as correct ranking. This ranking is reported in Table 2, along with the values of the Sobol indices.

Notably, the main drivers of the uncertainty on the reference PGA are m_{min} and σ_{GMPE}. While the dependence on σ_{GMPE} is a well-established result [52], the dependence on m_{min} is not that straightforward, and it is probably due to the selection of a target site in the very near field (about 10 km) and the use of a very large value for the slope b-value (about 2). The

combined effect of these two parameters is to produce a very large number of events with a magnitude very close to m_{min}, resulting in a critical dependence of the reference PGA on the selected minimum magnitude value. Also, notice that the estimates of the first order Sobol indices sum to greater than one, meaning that the variables considered are interacting (i.e., the source simulation code implements a non-linear model) [53]. Finally, it is worth mentioning that this result cannot be taken as general, because obtained under specific modelling assumptions (e.g., large return period and large PGA values): the analysis of the results to other settings/assumptions/constraints and the generality of such results is the object of future work.

Table 2 – Input variables ranking obtained with the standard GSA.

Rank	1	2	3	4	5	6
Input variable	m_{min}	σ_{GMPE}	λ	r	m_{max}	b
$\boldsymbol{S_n}$	0.5896	0.3811	0.0470	0.0320	0.0264	0.0221

4.1 RESULTS OF THE BOTTOM-UP STRATEGY

The application of the ensemble BU strategy produces the final ranking obtained by the Borda method, shown in Table 3. The major limitation of the BU strategy is that the result is lumped in a ranking table that is not transparent with respect to the actual Sobol indices that generate that ranking and, finally, the analyst is not provided with any confidence measure on the resulting rank: in other words, it cannot be quantitatively assessed how much the generic n-th input X_n contributes to the variance of Y.

Table 3 – Input variables ranking obtained through MGSA, D=1000 bootstrapped datasets, BU strategy.

Rank	1	2	3	4	5	6
Input variable	m_{min}	σ_{GMPE}	λ	r	m_{max}	b

4.2 RESULTS OF THE ALL-OUT STRATEGY

The ranking and the expected values of the Sobol indices obtained with the ensemble strategy AO are reported in Table 4. As stated for the BU strategy, one can observe that:

1. The variables σ_{GMPE} and m_{min} are the first two (by far) more relevant inputs (Figure 4);
2. The other input variables bring a negligible contribution to the variability of the output.

Table 4 – Input variables ranking obtained through MGSA, D=1000 bootstrapped datasets, AO strategy.

Rank	1	2	3	4	5	6
Input variable	m_{min}	σ_{GMPE}	λ	m_{max}	r	b
$\mathbb{E}(\boldsymbol{S_n})$	0.5760	0.3693	0.0508	0.0359	0.0336	0.0249

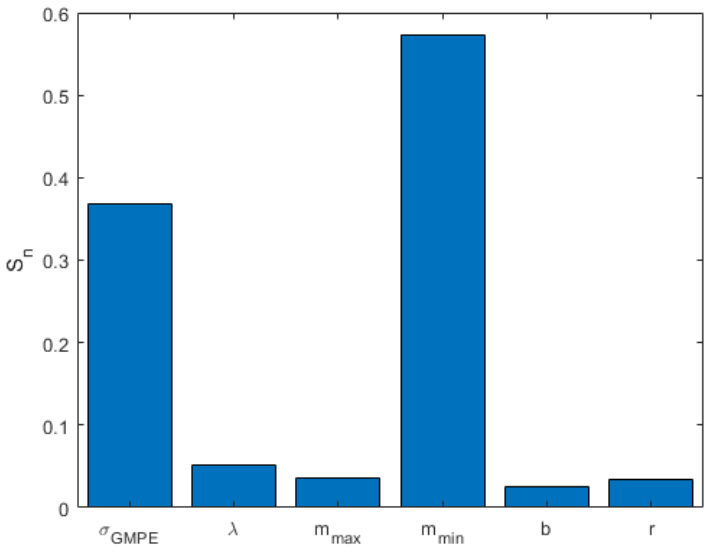

Figure 4 – Sobol indices obtained with the AO strategy.

4.3 COMPARISON WITH THE BENCHMARK RESULTS

The results of the proposed methodology have been then compared with the ranking results of the standard GSA, reported in Table 5.

Table 5 – Input variables rankings (sample size S=16384).

Rank	1	2	3	4	5	6
Standard GSA	m_{min}	σ_{GMPE}	λ	r	b	m_{max}
BU (BMGSA)	m_{min}	σ_{GMPE}	λ	m_{max}	r	b
AO (BMGSA)	m_{min}	σ_{GMPE}	λ	m_{max}	r	b
No bootstrap (MGSA)	m_{min}	σ_{GMPE}	r	m_{max}	λ	b

Both ensemble strategies and the standard GSA identify the σ_{GMPE} and m_{min} as the most important variables, whereas the sensitivity indices of the other input variables are negligible (Table 5, Figure 5). The disagreement regarding the ranking for the positions 4-6 may be due to the interactions between the input variables that might have been overlooked by the random alternative datasets generation, further exacerbated by the paucity of data upon which the rankings are drawn.

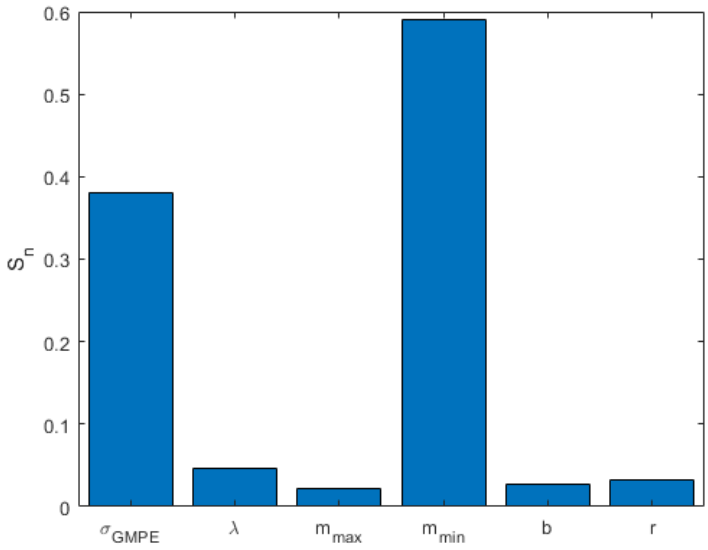

Figure 5 – Sobol indices obtained with the standard GSA.

To highlight the important role played by the bootstrapping (Section 2.2) in obtaining such results, we show (from Figure 6 to Figure 10) the results that would have been obtained with a given input-output dataset $\bar{\bar{Z}}$ of decreasing size ($S = 16384, 8192, 4096, 2048, 1024$) (that correspond to

successive halves of the dataset size), employing the more transparent AO ensemble strategy (green squares in Figure 6 to Figure 10). These results are compared with i) the benchmark values (Standard GSA, blue diamonds in the Figure 6 - Figure 10) and ii) the results obtained with the MGSA without bootstrap (magenta circles in the Figure 6 - Figure 10). The relative rankings are reported in Tables 6-9.

When $\bar{\bar{Z}} = [16384 \times 7]$ and $\bar{\bar{Z}} = [8192 \times 7]$, the Standard GSA (), the BMGSA (green squares in the Figure 6) and the MGSA agree on the identification of m_{min} and σ_{GMPE} as the most important variables, whereas for the third most important variable only Standard GSA and BMGSA agree on λ. Then, the approaches provide different rankings for lower ranking positions.

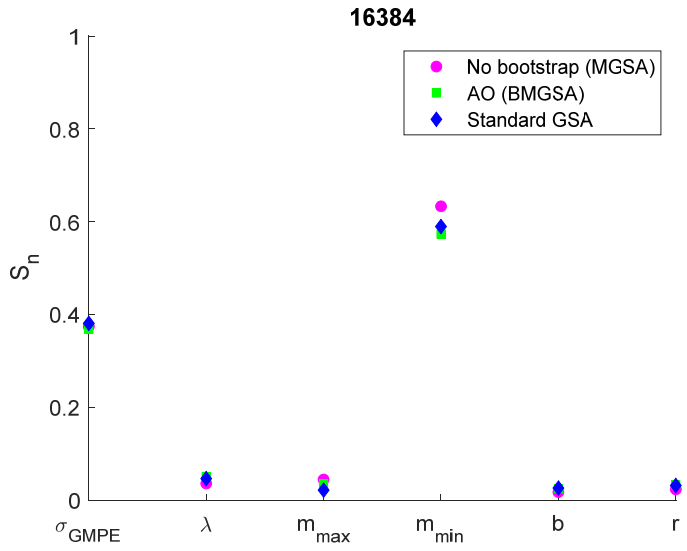

Figure 6 – Sobol indices estimates at sample size S=16384.

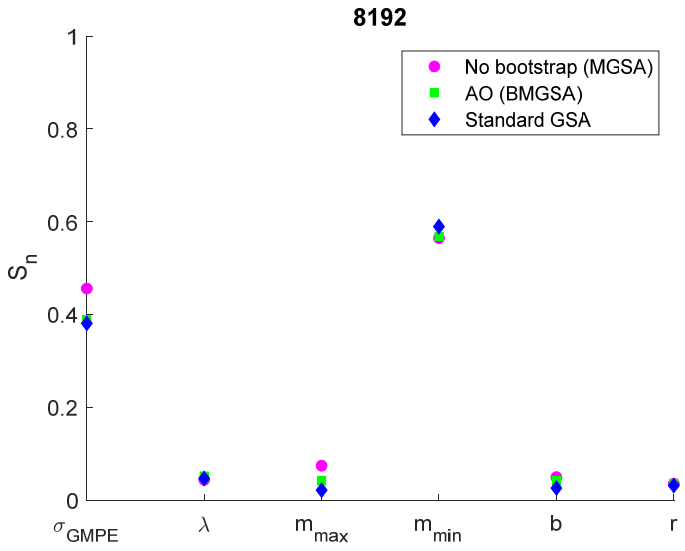

Figure 7 – Sobol indices estimates at sample size S=8192.

Table 6 – Input variables rankings (sample size S=8192).

Rank	1	2	3	4	5	6
Standard GSA	m_{min}	σ_{GMPE}	λ	r	b	m_{max}
AO (BMGSA)	m_{min}	σ_{GMPE}	λ	b	m_{max}	r
No bootstrap (MGSA)	m_{min}	σ_{GMPE}	m_{max}	b	λ	r

When $\bar{\bar{Z}} = [4096 \times 7]$ and $\bar{\bar{Z}} = [2048 \times 7]$, the Standard GSA and the BMGSA agree on the identification of m_{min} and σ_{GMPE} as the most important variables, as well as on the third (λ) and fourth (r) most important variables. Then, the approaches provide different rankings for lower ranking positions. The MGSA instead yields a completely different ranking (except for positions 4 and 5, when $\bar{\bar{Z}} = [4096 \times 7]$ and $\bar{\bar{Z}} = [2048 \times 7]$, respectively). Notice that, when the dimension of $\bar{\bar{Z}}$ decreases, even if the most important variables are correctly identified, a less accurate estimation of the Sobol indices is provided and the differences between the GSA, the BMGSA and MGSA increase.

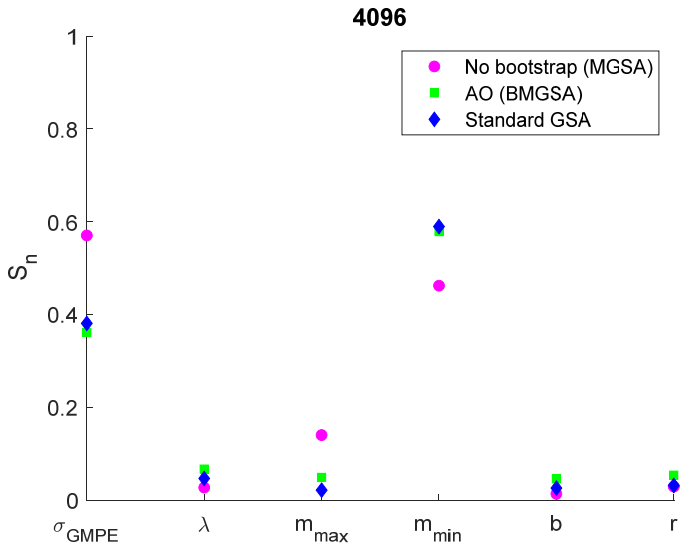

Figure 8 – Sobol indices estimates at sample size S=4096.

Table 7 – Input variables rankings (sample size S=4096).

Rank	1	2	3	4	5	6
Standard GSA	m_{min}	σ_{GMPE}	λ	r	b	m_{max}
AO (BMGSA)	m_{min}	σ_{GMPE}	λ	r	m_{max}	b
No bootstrap (MGSA)	σ_{GMPE}	m_{min}	m_{max}	r	λ	b

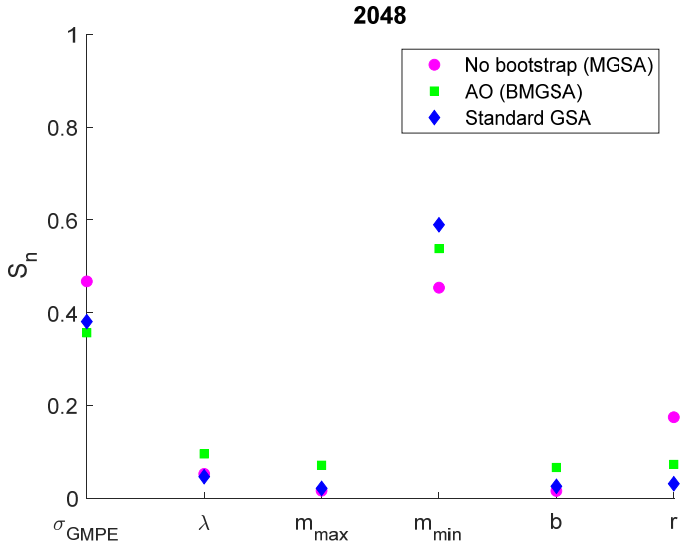

Figure 9 – Sobol indices estimates at sample size S=2048.

Table 8 – Input variables rankings (sample size S=2048).

Rank	1	2	3	4	5	6
Standard GSA	m_{min}	σ_{GMPE}	λ	r	b	m_{max}
AO (BMGSA)	m_{min}	σ_{GMPE}	λ	r	m_{max}	b
No bootstrap (MGSA)	σ_{GMPE}	m_{min}	r	λ	m_{max}	b

When $\bar{\bar{Z}} = [1024 \times 7]$, the Standard GSA, the BMGSA and the MGSA agree on the identification of m_{min} as the most important variable, whereas for the second (σ_{GMPE}) and third (λ) most important variables only Standard GSA and BMGSA agree. Then, the approaches provide different rankings for lower ranking positions. Nevertheless, as Figure 10 clearly shows, the numerical values of the Sobol indices obtained with the proposed BMGSA may not be considered satisfactory. Furthermore, Figure 11 to Figure 15 shows that, when the dimension of $\bar{\bar{Z}}$ decreases, the distributions of $S_{n,d}$ become wider (i.e., bootstrap replicates are subject to noise and, as a result, the Sobol indices estimate are not precise).

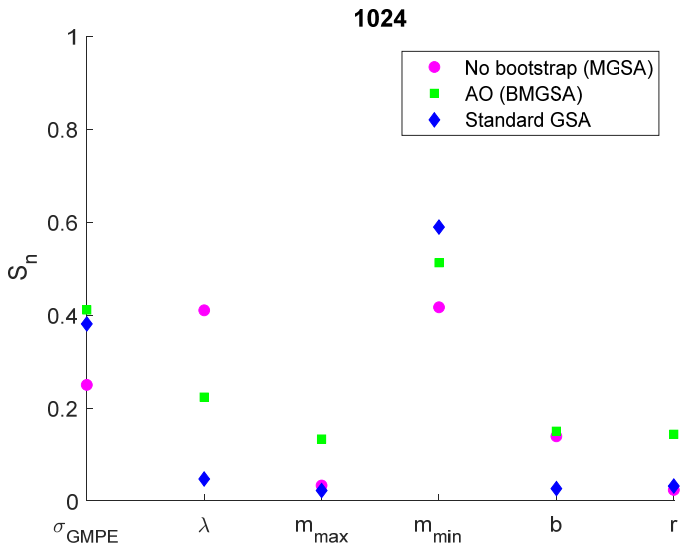

Figure 10 – Sobol indices estimates at sample size S=1024.

Table 9 – Input variables rankings (sample size S=1024).

Rank	1	2	3	4	5	6
Standard GSA	m_{min}	σ_{GMPE}	λ	r	b	m_{max}
AO (BMGSA)	m_{min}	σ_{GMPE}	λ	b	r	m_{max}
No bootstrap (MGSA)	m_{min}	λ	σ_{GMPE}	b	m_{max}	r

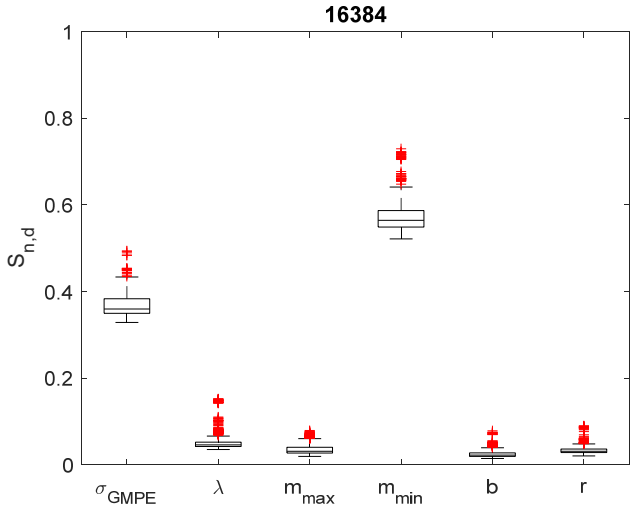

Figure 11 - $S_{n,d}$ distributions at sample size S=16384

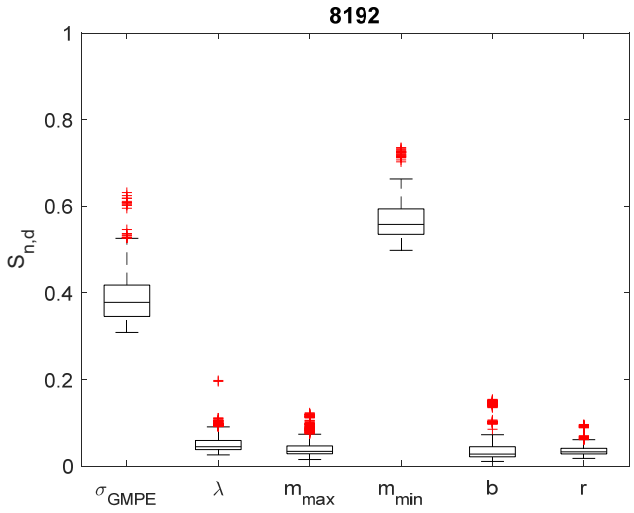

Figure 12 - $S_{n,d}$ distributions at sample size S=8192

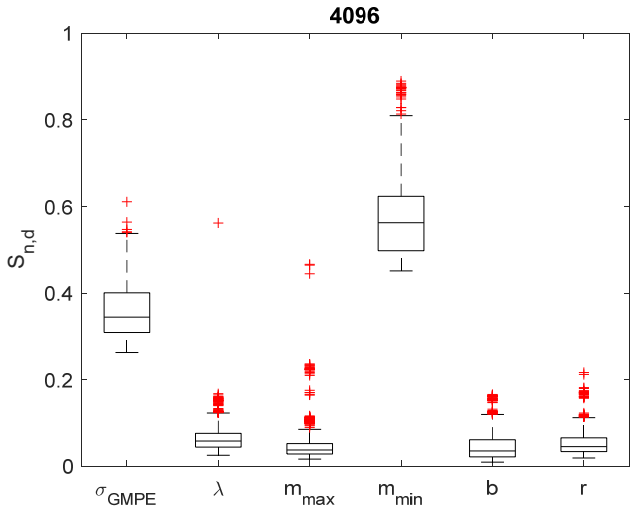

Figure 13 - $S_{n,d}$ distributions at sample size S=4096

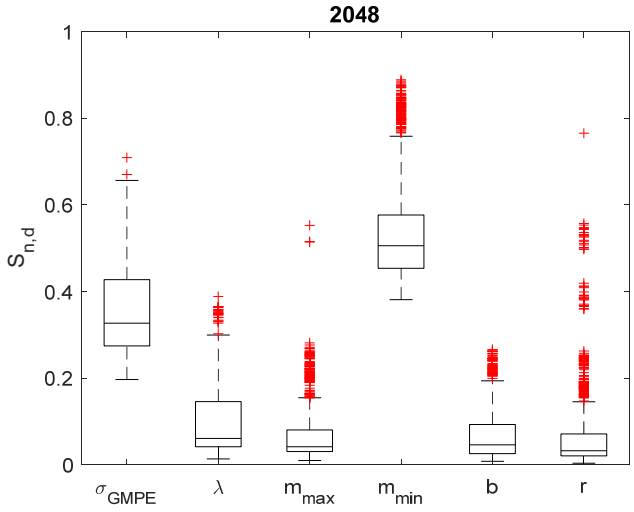

Figure 14 - $S_{n,d}$ distributions at sample size S=2048

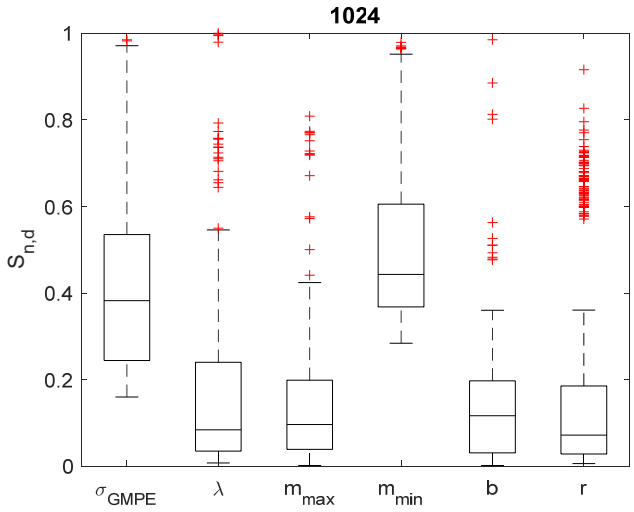

Figure 15 - $S_{n,d}$ distributions at sample size S=1024

As general conclusion, we can state that bootstrapping allows relying on a very small dataset. Indeed, a sample size of $S = 2048$ (Figure 9) allows correctly identifying the most important input variables, whereas $S = 4096$ (Figure 8) yields already a very satisfactory estimate of the Sobol indices values (compared with the GSA estimates). Thus, as a general recommendation, we may conclude that a ratio of 4:1 of $S{:}\,D$ (dataset size vs number of bootstrap replicates) is enough to guarantee satisfactory results, without resorting further to demanding computations.

For the case study at hand, we can conclude that, m_{min}, σ_{GMPE}, and λ have been identified as the input variables which most influence the reference PGA, whereas r, b, and m_{max} influence is negligible (for whatever dataset size $S = 16384, 8192, 4096, 2048, 1024$). The analyst, once identified the input parameters which most influence the uncertainty on reference PGA, may decide to further investigate the choice made regarding such inputs and proceed with the uncertainty analysis.

We underline that the numerical results obtained are relative to the specific case study and cannot be generalized to other PSHA cases. In particular, while the strong impact of σ_{GMPE}, and λ on hazard quantifications is well known (e.g. [13]), the reasons behind the importance of m_{min} must be further

investigated. In Figure 16, we show the impact of small events (i.e., with a magnitude around Mw 4.5). The relative short source-to-site distance (10 km) and the low PGA level (0.07g) make the contribution of small events of utmost relevance: the conditional probability of exceedance of such PGA level for a magnitude Mw 4.5 is larger than 0.2. In the case of larger distances (e.g., 40km) and larger PGA levels (e.g., 0.20g), the impact of small events decreases noticeably.

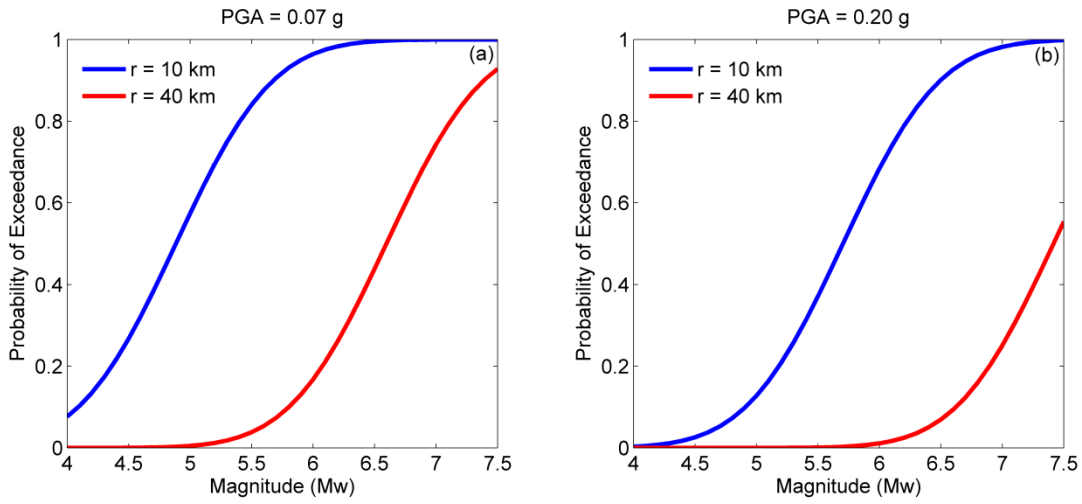

Figure 16 – Probability of exceedance of a specific PGA level, 0.07g for panel (a), 0.20g for panel (b), as a function of the magnitude, using the GMPE adopted in this study, for two different distances (10 km for the blue curve, 40 km for the red curve)

The large probabilities shown by the blue curve (r=10 km) in Figure 16 (a) explain the unexpected large importance of m_{min} as input variable in the PSHA computation (see [52] or [54]) and calls for a deeper investigation of the effect of small magnitude events in PSHA, as it is in the case of volcanic islands [42]. This highlights that the proposed method is useful to be used for sanity check of hazard assessments, as PSHA results are assumed independent from the selection of m_{min} [13]. In this case, indeed, we show that, for small magnitudes, the tails of the GMPE are sufficiently populated to strongly impact the hazard quantification also at a relatively high return period (475 years in this case), at least in the near field of the source areas.

Notably, this effect may be due to the extension of the validity of the GMPEs to small magnitude events that, in some cases, can even lead to a bias in the hazard estimation, as pointed out also in other studies (see [52], [54]),.

5. CONCLUSIONS

In this work, we have proposed a novel Bootstrapped Modularised Sensitivity Analysis (BMGSA) method based on bootstrapping, MGSA and ensemble strategies to identify the input parameters which the output of a PSHA model is most sensitive to, assuming that only an input-output dataset is given whereas the model is not available. The novelty and strength of the proposed BMGSA method is that to be applied it only needs data and not the source simulation code. The capability of the proposed method is tested on a benchmark case study. The results have been compared with a standard variance-based GSA method of literature, showing that the proposed method and the standard GSA agree on the identification of the three by-far most important input variables. Furthermore, the BMGSA has proved to be reliable even when applied to very small datasets.

The application of the developed technique to a realistic PSHA demonstrates its capability of scoring correctly the importance of existing uncertainty factor, needing only the input and the output data. This allows applying the technique to any hazard model in which uncertainty is to be evaluated. Its systematic application to hazard studies to detect the most influential parameters would allow hazard practitioners to both improve the sanity checks during the assessment and to focus future research toward the reduction of uncertainty, by further characterisation of the important factors. The results of our applications, for example, highlight the importance of small magnitudes near to the seismic source areas, showing the importance of the definition of the minimum magnitude and the potential impact of the tail of the uncertainty distributions on GMPE on seismic hazard evaluation. Also, the application of the proposed technique can result practically useful when the PSHA is to be updated on a time basis (usually 5/10 years): in this case, a standard GSA would not allow the seismologist to obtain the results in reasonable time; on the contrary, the BMGSA here proposed enables a lean update of the PSHA, by informing the seismologists about the parameters

that rule most the uncertainty; focusing on these only, scenarios exploration and conclusions would be more swiftly performed and drawn, respectively.

Acknowledgments

This study was developed within the research project “Assessment of Cascading Events triggered by the Interaction of Natural Hazards and Technological Scenarios involving the release of Hazardous Substances” funded by MIUR - Italian Ministry for Scientific Research under the PRIN 2017 program (grant 2017CEYPS8).

References

[1] R. K. Mcguire, “Probabilistic seismic hazard analysis: Early history , vol. 37,” *Earthq. Eng. Struct. Dyn. Earthq. Engng Struct. Dyn,* p. 329–338, 2008.

[2] C. A. Cornell, “Engineering seismic risk analysis,” *Bulletin of the seismological society of America,* vol. 58, no. 5, pp. 1583-1606, 1968.

[3] C. Meletti, F. Galadini, G. Valensise, M. Stucchi, R. Basili, S. Barba, G. Vannucci and E. Boschi, “A seismic source zone model for the seismic hazard assessment of the Italian territory,” *Tectonophysics,* vol. 450, pp. 85-108, 2008.

[4] A. Frankel, “Mapping seismic hazard in the central and eastern United States,” *Seismological Research Letters,* vol. 66, no. 4, pp. 8-21, 1995.

[5] E. Chioccarelli, P. Cito, F. Visini and I. Iervolino, “Sequence-based hazard analysis for Italy considering a grid seismic source model,” *Annals of Geophysics,* vol. 64, no. 2, 26 May 2021.

[6] P. Cito, E. Chioccarelli and I. Iervolino, “Macroseismic intensity hazard maps for Italy based on a recent grid source model,” *Bulletin of Earthquake Engineering,* vol. 20, pp. 2245-2258, 2022.

[7] B. Gutenberg and C. F. Richter, “Frequency of earthquakes in California,” *Bulletin of the Seismological society of America,* vol. 34, no. 4, pp. 185-188, 1944.

[8] J. Selva and L. Sandri, “Probabilistic seismic hazard assessment: Combining Cornell-like approaches and data at sites through Bayesian inference,” *Bull. Seismol. Soc. Am., vol. 103, no. 3,* p. 1709–1722, June 2013.

[9] R. K. McGuire and W. J. W. J. Arabasz, “12. An Introduction to Probabilistic Seismic Hazard Analysis,” 1990, p. 333–354.

[10] M. Kowsari, N. Eftekhari, A. Kijko, E. Yousefi Dadras, H. Ghazi and E. Shabani, “Quantifying Seismicity Parameter Uncertainties and Their Effects on Probabilistic Seismic Hazard Analysis: A Case Study of Iran,” *Pure Appl. Geophys., vol. 176, no. 4,* pp. 1487-1502, April 2019.

[11] L. Hofer and M. A. Zanini, “The role of uncertainty of model parameters in PSHA,” *COMPDYN Proceedings,* vol. 3, p. 5527–5534, 2019.

[12] F. Di Maio, A. Bandini, E. Zio, S. C. Alberola, F. Sanchez-Saez and S. Martorell, “Bootstrapped-ensemble-based Sensitivity Analysis of a trace thermal-hydraulic model based on a limited number of PWR large break loca simulations,” *Reliab. Eng. Syst. Saf.,* vol. 153, pp. 122-134, September 2016.

[13] C. Molkenthin, F. Scherbaum, A. Griewank, H. Leovey, S. Kucherenko and F. Cotton, “Derivative-based global sensitivity analysis: Upper bounding of sensitivities in seismic-hazard assessment using automatic differentiation,” *Bull. Seismol. Soc. Am.,* vol. 107, no. 2, pp. 984-1004, April 2017.

[14] F. Cadini, S. S. Lombardo and M. Giglio, “Global reliability sensitivity analysis by Sobol-based dynamic adaptive kriging importance sampling,” *Struct. Saf.,* vol. 87, p. 101998, November 2020.

[15] E. Borgonovo and E. Plischke, “Sensitivity analysis: A review of recent advances,” *European Journal of Operational Research,* vol. 248, no. 3, p. 869–887, 01 February 2016.

[16] E. Zio, Computational Methods for Reliability and Risk Analysis, 2009.

[17] A. Saltelli and al., Global Sensitivity Analysis. The Primer., 2008.

[18] A. Saltelli and J. Marivoet, “Non-parametric statistics in sensitivity analysis for model output: A comparison of selected techniques,” *Reliab. Eng. Syst. Saf.,* vol. 28, no. 2, p. 229–253, January 1990.

[19] M. Menz, S. Dubreuil, J. Morio, C. Gogu, N. Bartoli and M. Chiron, “Variance based sensitivity analysis for Monte Carlo and importance sampling reliability assessment with Gaussian processes,” *Struct. Saf.,* vol. 93, p. 102116, November 2021.

[20] L. Li, I. Papaioannou and D. Straub, “Global reliability sensitivity estimation based on failure samples,” *Struct. Saf.,* vol. 81, p. 101871, November 2019.

[21] E. Borgonovo, “A new uncertainty importance measure,” *Reliab. Eng. Syst. Saf.,* vol. 92, no. 6, p. 771–784, June 2007.

[22] Q. Liu and T. Homma, “A new computational method of a moment-independent uncertainty importance measure,” *Reliab. Eng. Syst. Saf.,* vol. 94, no. 7, pp. 1205-1211, July 2009.

[23] J. E. Oakley, A. Brennan, P. Tappenden and J. Chilcott, “Simulation sample sizes for Monte Carlo partial EVPI calculations,” *J. Health Econ.,* vol. 29, no. 3, p. 468–477, May 2010.

[24] Z. Hu and S. Mahadevan, “Probability models for data-Driven global sensitivity analysis,” *Reliab. Eng. Syst. Saf.,* vol. 187, p. 40–57, July 2019.

[25] E. Plischke, “An adaptive correlation ratio method using the cumulative sum of the reordered output,” *Reliability Engineering and System Safety,* vol. 107, p. 149–156, 2012.

[26] C. Li and S. S. Mahadevan, “An efficient modularized sample-based method to estimate the first-order Sobol index,” *Reliab. Eng. Syst. Saf.,* vol. 153, p. 110–121, Sep. 2016.

[27] E. Plischke, E. Borgonovo and C. L. Smith, “Global sensitivity measures from given data,” *Eur. J. Oper. Res.,* vol. 226, no. 3, p. 536–550, May 2013.

[28] J. E. Oakley and A. O’Hagan, “Probabilistic sensitivity analysis of complex models: A Bayesian approach,” *J. R. Stat. Soc. Ser. B Stat. Methodol.,* vol. 66, no. 3, p. 751–769, 2004.

[29] J. P. C. Kleijnen, “Kriging metamodeling in simulation: A review,” *European Journal of Operational Research,* vol. 192, no. 3, p. 707–716, 01 February 2009.

[30] B. Sudret, “Global sensitivity analysis using polynomial chaos expansions,” *Reliability Engineering and System Safety,* vol. 93, no. 7, p. 964–979, 01 July 2008.

[31] Y. Caniou and B. Sudret, “Distribution-based global sensitivity analysis using polynomial chaos expansions,” *Procedia - Social and Behavioral Sciences,* vol. 2, no. 6, p. 7625–7626, 2010.

[32] S. Tarantola, D. Gatelli and T. A. Mara, “Random balance designs for the estimation of first order global sensitivity indices,” *Reliab. Eng. Syst. Saf.,* vol. 91, no. 6, p. 717–727, June 2006.

[33] C. Xu and G. Gertner, “Extending a global sensitivity analysis technique to models with correlated parameters,” *Comput. Stat. Data Anal.,* vol. 51, no. 12, p. 5579–5590, August 2007.

[34] E. Plischke, “An effective algorithm for computing global sensitivity indices (EASI),” *Reliab. Eng. Syst. Saf.,,* vol. 95, no. 4, p. 354–360, April 2010.

[35] M. Strong and J. E. J. E. Oakley, “An efficient method for computing single-parameter partial expected value of perfect information,” *Med. Decis. Mak.,* vol. 33, no. 6, p. 755–766, 2013.

[36] Y. J. Lai, T. Y. Liu and C. L. Hwang, “TOPSIS for MODM,” *Eur. J. Oper. Res.,* vol. 76, no. 3, p. 486–500, August 1994.

[37] Z. Liu and Y. Choe, “Data-driven sensitivity indices for models with dependent inputs using polynomial chaos expansions,” *Struct. Saf.,,* vol. 88, p. 101984, January 2021.

[38] E. Borgonovo, X. Lu, E. Plischke, O. Rakovec and M. C. Hill, “Making the most out of a hydrological model data set: Sensitivity analyses to open the model black-box,” *Water Resour. Res.,* vol. 53, no. 9, p. 7933–7950, September 2017.

[39] Y. Y. Kagan, “Seismic moment distribution revisited: I. Statistical results,” *Geophysical Journal International,* vol. 148, no. 3, pp. 520-541, March 2002.

[40] S. M. Hoseyni, F. Di Maio, M. Vagnoli, E. Zio and M. Pourgol-Mohammad, “A Bayesian ensemble of sensitivity measures for severe accident modeling,” *Nucl. Eng. Des.,* vol. 295, p. 182–191, Dec. 2015.

[41] J. P. C. Kleijnen and D. Deflandre, “Validation of regression metamodels in simulation: Bootstrap approach,” *Eur. J. Oper. Res.,* vol. 170, no. 1, p. 120–131, Apr. 2006.

[42] J. Selva, R. Azzaro, T. M. A. Tramelli, G. Alessio, M. Castellano, C. Ciuccarelli, E. Cubellis, D. Lo Bascio, S. Porfido, P. Ricciolino and A. Rovida, “The Seismicity of Ischia Island, Italy: An Integrated Earthquake Catalogue From 8th Century BC to 2019 and Its Statistical Properties,” *Frontiers in Earth Science,* vol. 9, p. 629736, 8 April 2021.

[43] P. Baraldi, G. Gola, E. Zio, D. Roverso and M. Hoffmann, “A randomized model ensemble approach for reconstructing signals from faulty sensors,” *Expert Syst. Appl.,* vol. 38, no. 8, p. 9211–9224, Aug. 2011.

[44] P. Baraldi, E. Zio, G. Gola, D. Roverso and M. Hoffmann, “Two novel procedures for aggregating randomized model ensemble outcomes for robust signal reconstruction in nuclear power plants monitoring systems,” *Ann. Nucl. Energy,* vol. 38, no. 2-3, p. 212–220, February 2011.

[45] T. Homma and A. Saltelli, “Importance measures in global sensitivity analysis of nonlinear models,” *Reliab. Eng. Syst. Saf.,* vol. 52, no. 1, pp. 1-17, 1996.

[46] F. Maio, G. Nicola, Y. Yu, E. Zio and F. Di Maio, “Sensitivity Analysis and Failure Damage Domain Identification of the Passive Containment Cooling System of an AP1000 Nuclear Reactor,” 2014.

[47] M. Strong, J. E. Oakley and J. Chilcott, “Managing structural uncertainty in health economic decision models: A discrepancy approach,” *J. R. Stat. Soc. Ser. C Appl. Stat.,* vol. 61, no. 1, p. 25–45, Jan. 2012.

[48] C. Cauzzi and E. Faccioli, “Broadband (0.05 to 20 s) prediction of displacement response spectra based on worldwide digital records,” *Journal of Seismology,* vol. 12, p. 453, 2008.

[49] G. Lanzano and L. Luzi, “A ground motion model for volcanic areas in Italy,” *Bulletin of Earthquake Engineering,* vol. 18, pp. 57-76, 2020.

[50] M. Stucchi, A. Akinci, E. Faccioli, P. Gasperini, L. Malagnini, C. Meletti, V. Montaldo and G. Valensise, “Redazione della mappa di pericolosità sismica prevista dall’Ordinanza PCM del 20 marzo 2003. Rapporto Finale,” Istituto Nazionale di Geofisica e Vulcanologia, Milano, 2003.

[51] M. Stucchi, C. Meletti, V. Montaldo, H. Crowley, G. M. Calvi and E. Boschi, “Seismic hazard assessment (2003-2009) for the Italian building code,” *Bull. Seismol. Soc. Am.,* vol. 101, no. 4, p. 1885–1911, Aug. 2011.

[52] J. J. Bommer and N. A. Abrahamson, “Why do modern probabilistic seismic-hazard analyses often lead to increased hazard estimates?,” *Bulletin of the Seismological Society of America,* vol. 96, no. 6, p. 1967–1977, December 2006.

[53] E. Zio, “BASIC CONCEPTS OF UNCERTAINTY AND SENSITIVITY ANALYSIS,” in *Computational Methods for Reliability and Risk Analysis*, Series on Quality, Reliability and Engineering StatisticsComputational Methods for Reliability and Risk Analysis, WorldScientific, 2009, p. 295–340.

[54] R. M. W. Musson, “Ground motion and probabilistic hazard,” *Bull. Earthq. Eng.,* vol. 7, no. 3, p. 575–589, August 2009.